工學碩士 學位論文

A Very Compact Miniaturized GaAs Bandpass Filter For 5GHz Band WLAN

5GHz WLAN 용 초소형 GaAs 대역 통과 필터

指導教授 姜 仁 鎬

2007 年 8 月

韓國海洋大學校 大學院

電 波 工 學 科

單 世 偉

工學碩士 學位論文

A Very Compact Miniaturized GaAs Bandpass Filter For 5GHz Band WLAN

5GHz WLAN 용 초소형 GaAs 대역 통과 필터

指導教授 姜 仁 鎬

2007年 8月

韓國海洋大學校 大學院

電 波 工 學 科

單 世 偉

本 論文을 單世偉의 工學碩士 學位論文으로 認准함.

위원장 : 공학박사 조 형 래 (인)

위 원 : 공학박사 윤 영 (인)

위 원 : 공학박사 강 인 호 (인)

2007 년 6 월

한 국 해 양 대 학 교 대 학 원

Contents

Nomenclature

f	:	Frequency
f_0	:	Center frequency
Q	:	Quality factor
C	:	Capacitance
λ	:	Wave-length
SIR	:	Step impedance filter
MMIC	:	Monolithic microwave integrated circuit
MIM	:	Metal-Insulator-Metal
Z_0	:	Characteristic Impedance
Z_{oe}	:	Even mode impedance
Z_{oo}	:	Odd mode impedance
Y	:	Characteristic admittance
θ	:	Electrical length
$\boldsymbol{S}_{ij}(i = j)$	:	Reflection coefficient
$\boldsymbol{S}_{ij}(i \neq j)$	:	Transmission coefficient
K	:	Coupling coefficient

List of Figures

Abstract

Shiwei Shan

Dept. of Radio Science & Engineering

Graduate School, Korea Maritime Univ.

Supervisor: Prof. In-ho Kang, Ph.D

Bandpass filters are often used in microwave systems, especially in the modern wireless communication system. Microwave bandpass filters with compact size, low cost, good stopband and monolithic integration for single transceiver chip are required because the limited space is allowed for most mobile platforms.

In this thesis, a very compact GaAs bandpass filter using a combination of end shorted parallel coupled lines and lumped capacitors was designed, fabricated and measured. Using the above structure, the electrical length of the parallel coupled lines in the GaAs filter, which determines the size of a GaAs filter, can be reduced to even a few degrees, resulting in a much smaller circuit area. Inter-stage connecting lines have been added to connect the neighboring resonators for the suppression of unwanted coupling which play an important role as an indispensable component. In addition to it, the designed GaAs filter also shows a wide upper stopband.

After fabrication, the real size of the bandpass filter is extremely

small, just about $0.54 \times 0.78 mm^2$. Measured results of a fabricated filter centered at about 5 GHz also show good agreement with the theoretical predications.

요 약

Shiwei Shan
학 교 : 한 국 해 양 대 학 교
학 과 : 전 파 공 학 과
지도교수 : 강 인 호

대역통과필터는 마이크로파시스템에서 특히 현대 무선 통신 시스템에서 많이 응용하고 있다. 대부분의 이동통신 시스템에서 단일 송수신 칩 구현을 위하여 작은 사이즈와 낮은 가격, 그리고 저지대역에서 높은 감쇠특성을 가지는 MMIC 대역통과 필터를 필요로 한다.

본 논문에서 종단 단락 된 평행 결합선과 집중 capacitor 를 이용하여 새로운 소형화된 GaAs 대역 통과필터를 제안 하였다. 위에 언급하여 제안한 구조를 이용하여 GaAs 필터의 사이즈는 GaAs 필터에 있은 평행결합선의 전기적인 길로 결정할 수 있다. 그래서 평행 결합선의 길을 줄이는 방법을 통하여 매우 작은 필터를 구성할 수 있은 것이다. 불필요한 신호를 억제하기 위해서 inter-stage 선로를 서로 이웃한 공진기의 사이에서 삽입한다. 이 inter-stage 선로는 반드시 필요한 회로 부분으로 중요한 역할을 하고 있다. 그리고 설계된 GaAs 필터는 넓은 높은 저지대역폭을 가지고 있다. 제작된 대역통과필터의 실제 size 는 $0.54\times0.78mm^2$ 까리 초소형화 되었다. 필터를 제작해서 측정된 결과는 본문에서 설계된 이론치와 잘 일치하였다.

Chapter 1 Introduction

In modern wireless communication systems, radio technologies have made evolved to multi frequency, multifunction, and multi-standard architectures. Microwave bandpass filters with compact size, low cost, good stop band and monolithic integration for single transceiver chip are required because the limited space is allowed for most mobile platforms. Many studies on reducing the size of bandpass filter have been made. To reduce the size, step impedance resonator (SIR) filters [1]-[3] and slow wave filters [4] were developed. In spite of small size and simple planar structure of these filters, they take up quite a large area.

Comb-line filters using low temperature co-fired ceramic (LTCC) or ceramic materials with the multi-layer technology can be used as reduced size [5], [6]. However, these filters can not be easily fabricated by commercial MMIC process due to 3-dimensional structure and low relative permittivity, compared with high one of ceramic filter. SAW filters are widely used in the mobile communication market. They are still not compatible with standard IC technology and presently available in the frequency range up to 3GHz [7]. An active bandpass filter can be integrated in one singe manufacturing process. In this case, the active circuit which behaves as a negative resistance is inserted [8] and has a drawback associated with nonlinearity and poor noise figures [9].

In this paper, GaAs process-based MMIC filter will be introduced for the RF single transceiver chip. It is composed of simple planar diagonally end-shorted coupled line and lumped capacitors.

The main advantages of this MMIC filter are as follows. The electrical length of resonator in MMIC filter can be reduced as small as a few degrees. The most chip filter using this concept can be designed to be smaller than $2 \times 1 \text{ mm}^2$. The spurious stopband can be expanded up to above 10 times center frequency. This property will be most powerful as the image rejection filter in the transceiver system. This technology is available to any kinds of standard fabrication process because the topology of this filter circuit is only planar two dimensional structures. Finally, it is also broadly applicable from IF to millimeter band because the electrical length of it can be arbitrarily controlled.

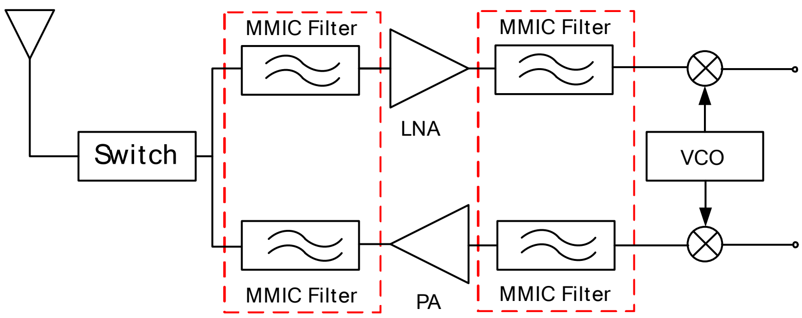

Fig.1.1 The transceiver chip model.

A filter using the GaAs process technology for single transceiver chip is designed and fabricated at 5.5GHz to maximize the effect of size reduction method because SAW filter covers the frequencies below 3GHz and ceramic filter is still too large to insert in RF transceiver system. Simulation and measurement results are also provided to verify this very compact miniaturized GaAs bandpass filter.

The contents of the thesis are illustrated as follows:

Chapter 1 briefly introduces the outline of this thesis, the background and the purpose of this work.

Chapter 2 presents a size reduction method for the Quarter-wavelength Transmission Line. This new method utilizes combinations of diagonally end-shorted coupled lines and shunt lumped capacitors. This chapter also explains the key factors which effect on the bandwidth of the filter.

Chapter 3 describes a design of two-stages bandpass filter in detail, including theoretical analysis, circuit design and simulated results by ADS and HFSS.

Chapter 4 shows the simulated results. The experimental results of the fabricated filter are also demonstrated and discussed.

Chapter 5 is the conclusion of this thesis. It summarizes the research work and proposes applications of this new type of filters.

Chapter 2 Size Reduction Method for the Quarter-wavelength Transmission Line

2.1 Introduction

A microwave filter is a two-port network used to control the frequency response at a certain point in a microwave system by providing transmission at frequencies within the passband of the filter and attenuation in the stopband of the filter. It is well known that they can be divided into four types of filters in RF and microwave system mainly in terms of frequency selectivity characteristics, such as Low-Pass Filter (LPF), High-Pass Filter (HPF), Band-Pass Filter (BPF), and Band-Stop Filter (BSF). Their representative frequency responses are shown in Fig.2.1.

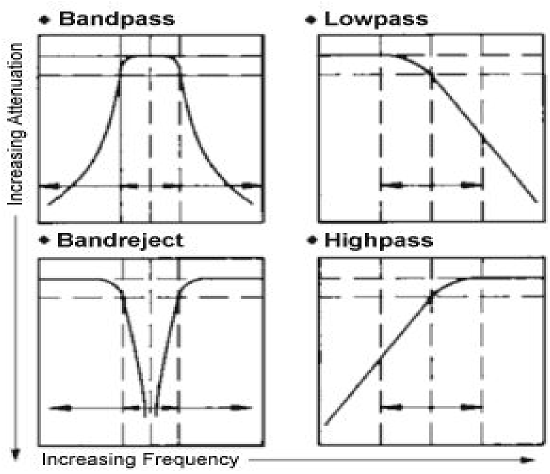

Fig.2.1 The classification in terms of frequency responses.

The low-pass filter allows low-frequency signals to be transmitted from the input to the output port with little attenuation. However, as the frequency exceeds a certain cut-off point, the attenuation increases significantly with the result of delivering an amplitude-reduced signal to the output port. The opposite behavior is true for a high-pass filter, where the low-frequency signal components are highly attenuated or reduced in amplitude, while beyond a cut-off frequency point the signal passes the filter with little attenuation. Bandpass and bandstop filters restrict the passband between specific lower and upper frequency points where the attenuation is either low (bandpass) or high (bandstop) compared to the remaining frequency band.

If following the different implementation methods of filters, there are two main kinds of filters, such as lumped-elements and distributed-elements filters. Lumped-elements filters are frequently applied in low-frequency band because the wavelength of the operation signal will be comparable to the size of the lump-elements itself, whereas the distributed-elements filters can be used in high-frequency band extending to decades and hundreds of gigahertz.

Filters have become indispensable devices not only in the field of telecommunication, but also in many other types of electrical equipment. Due to the variety and diversity of the filter types, it often becomes necessary for a designer to carefully consider which filter to adopt for a particular application.

2.2 Size Reduction Method

Miniaturized microwave bandpass filters are always in demand for systems requiring small size and light weight. This demand is much increased recently by rapidly expanding cellular communication systems. Although parallel–coupled microstrip filters with half-wavelength resonators are common elements in many microwave systems, their large size is incongruous with the systems where the size reduction is an important factor.

The planar filter structures which can be fabricated using printed-circuit technologies would be preferred whenever they are available and are suitable because of smaller size and lighter weight. The $\lambda/2$ hairpin resonator and slow-wave resonator filters of planar structure are not only compact size, but also have a wider upper stopband. However, this type of filters is still too large to be inserted into commercial transceiver system. Although the lumped-element approach, which uses spiral inductors and lumped capacitors, leads to small circuit size, they suffer from higher loss and poorer power handling capability.

The size-reduction method proposing by Hirota is attractive in view of using shorted transmission line and lumped capacitors. However, the circuit size could not be much reduced due to the limitation of the high impedance of the transmission line. It is therefore desirable to develop new types of microstrip bandpass filters which actually meet the requirement of small size.

2.3 Hirota's size reduction method for λ/4 transmission line

The reduced λ/4 transmission line using combinations of shortened transmission line and shunt lumped capacitors proposed by Hirota is shown in Fig.2.2. A transmission line shorter than a quarter of a wavelength has a lower inductance and capacitance. The approach is to offset the inductance drop by increasing the characteristic impedance of the transmission line and to offset the capacitance loss by adding lumped capacitors. The **ABCD**-matrices of the circuits in Fig. 2.2 (a) and (b) are as follows,

$$\left[\mathbf{ABCD}\right] = \begin{bmatrix} 0 & jZ_0 \\ \dfrac{j}{Z_0} & 0 \end{bmatrix} \tag{2.1}$$

$$\left[\mathbf{ABCD}\right] = \begin{bmatrix} 1 & 0 \\ j\omega C_1 & 1 \end{bmatrix} \begin{bmatrix} \cos\theta & jZ\sin\theta \\ j\dfrac{\sin\theta}{Z} & \cos\theta \end{bmatrix} \begin{bmatrix} 1 & 0 \\ j\omega C_1 & 1 \end{bmatrix}$$

$$= \begin{bmatrix} \cos\theta\text{-}\omega C_1 Z\sin\theta & jZ\sin\theta \\ j\dfrac{\sin\theta}{Z} + 2j\omega C_1\cos\theta\text{-}j(\omega C_1)^2 Z\sin\theta & \cos\theta\text{-}\omega C_1 Z\sin\theta \end{bmatrix} \tag{2.2}$$

where Z_0, Z, θ, ω, C_1 are the characteristic impedance of the λ/4 line, the characteristic impedance of the shortened line, the electrical length of the shortened line, the angular frequency, and the shunt capacitor, respectively.

Then we obtain the relation equations as follows:

$$Z = Z_0 / \sin\theta \tag{2.3}$$

$$\omega C_1 = \left(1/Z_0\right)\cos\theta \tag{2.4}$$

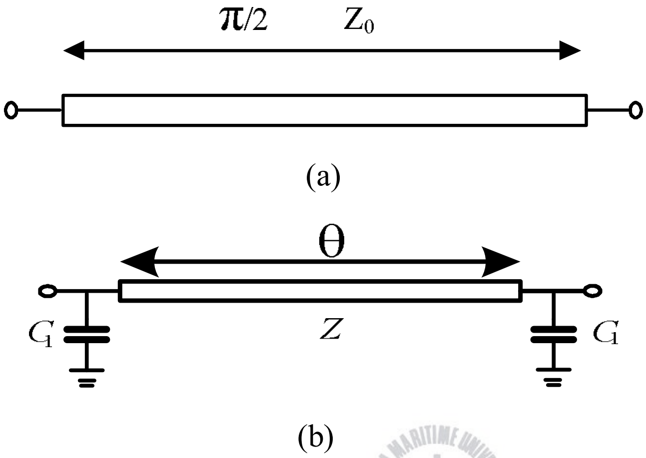

Fig.2.2 (a) The λ/4 transmission line. (b) Shortened transmission line equivalent to the λ/4 transmission line.

From equation (2.3), the characteristic impedance Z inclines to be higher as the electrical length θ goes smaller. But if θ is very small, Z will become too high to attain. As far as to now, the limitation of the electrical length of the transmission line is about λ/8 ~λ/12. Therefore, it is necessary to overcome the high impedance of the shortened transmission line.

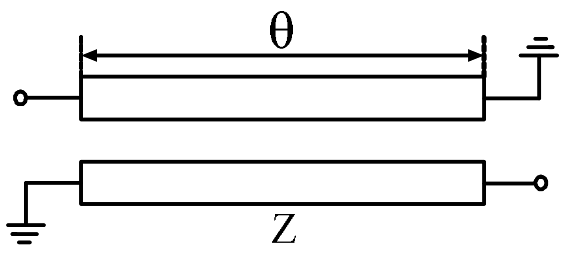

(a)

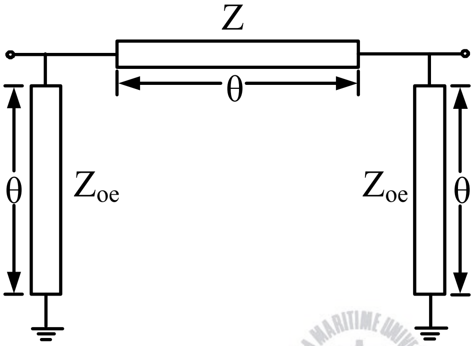

(b)

Fig.2.3 (a) Diagonally end-shorted coupled lines. (b) Equivalent circuit of the coupled lines.

Fig.2.3 (a) and (b) show the diagonally shorted coupled lines and its equivalent circuit. The **ABCD**-matrix of the circuits is,

$$\left[\mathbf{ABCD}\right]=\begin{bmatrix}1 & 0\\ \dfrac{1}{jZ_{oe}\tan\theta} & 1\end{bmatrix}\begin{bmatrix}\cos\theta & jZ\sin\theta\\ j\dfrac{\sin\theta}{Z} & \cos\theta\end{bmatrix}\begin{bmatrix}1 & 0\\ \dfrac{1}{jZ_{oe}\tan\theta} & 1\end{bmatrix} \qquad (2.5)$$

After calculation, the characteristic impedance of the diagonally shorted coupled lines is given by:

$$Z = \frac{2 Z_{oe} Z_{oo}}{Z_{oe} - Z_{oo}} \tag{2.6}$$

We can see from the equation (2.6) that the shorted coupled lines are proper for extremely miniaturized λ/4 transmission line as the high characteristic impedance can be easily achieved by choosing Zoe ≈ Zoo.

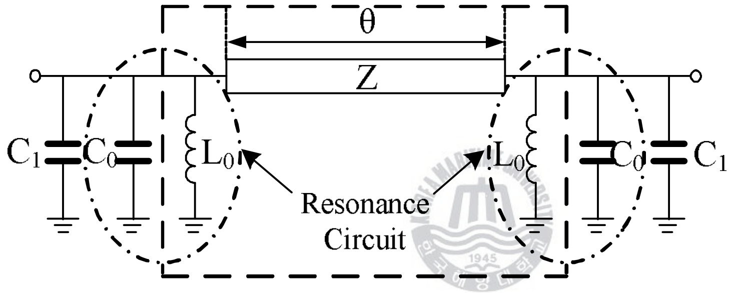

(a)

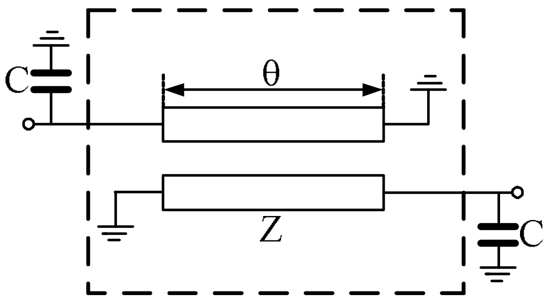

(b)

Fig.2.4 (a) Equivalent circuit of Hirota's reduced-size λ/4 line including artificial resonance circuits. (b) The final equivalent λ/4 transmission line circuit.

In Fig.2.4 (a), the artificial resonance circuits are inserted to Hirota's lumped distributed λ/4 transmission line. The high impedance transmission line with shunt lumped inductors can be replaced by coupled lines shown in Fig.2.4 (b). The parts in two dotted square boxes are equivalent when the following equations are satisfied:

$$\omega L_0 = Z_{oe} \tan\theta \tag{2.7}$$

$$\omega L_0 = \frac{1}{\omega C_0} \tag{2.8}$$

$$\mathrm{C} = \mathrm{C}_0 + \mathrm{C}_1 \tag{2.9}$$

The final miniaturized λ/4 transmission line is shown in Fig.2.4 (b). It is feasible to obtain very high impedance using coupled lines. The peculiar feature of this extremely miniaturized λ/4 transmission line is that resonance circuits are located at edge side of the transmission line. When the miniaturized λ/4 transmission lines are connected in series, the cascade circuit becomes a typical bandpass filter, with the λ/4 section as an admittance inverter. The circuit and its principle circuit show in the Fig.2.5.

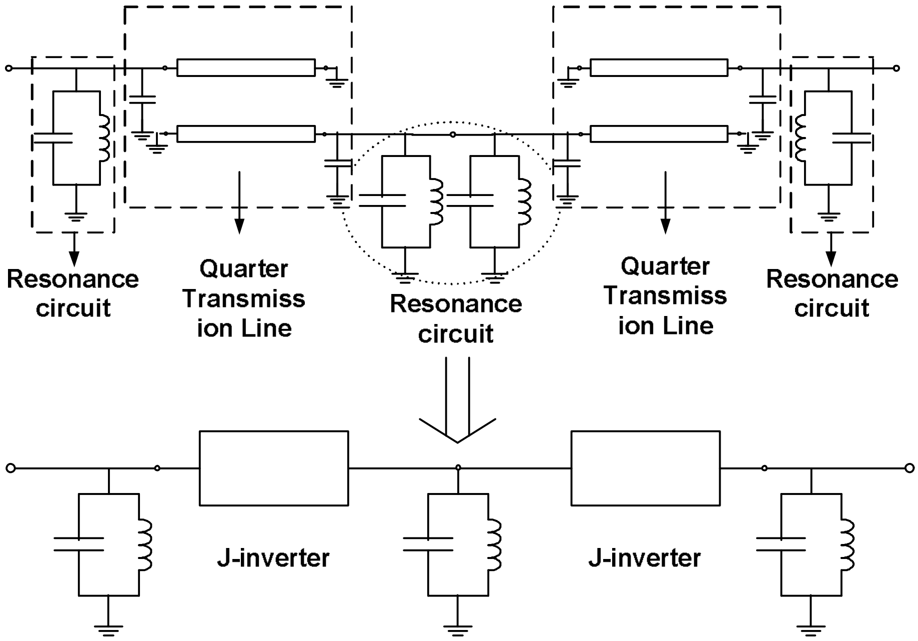

Fig.2.5 The equivalent bandpass filter.

The bandwidth of the filter can be controlled by the coupling coefficient since the bandwidth of diagonally end-shorted coupled line is closely related to the coupling coefficient [10].

Chapter 3 Bandpass Filter Design Theory

3.1 Introduction

The filter we studied here is based on a generalized bandpass filter model provided by [11], as shown in Fig.3.1, where $B_n(\omega)$ (n=1~N) represents resonant circuits and J_{0n} (n=1~N) admittance inverters. An idealized admittance inverter operates like a quarter-wavelength line of characteristic admittance J at all frequencies. Thus, if admittance Y_b is attached at one end, the admittance Y_a seen looking in the other end is:

$$Y_a = \frac{J^2}{Y_b} \tag{3.1}$$

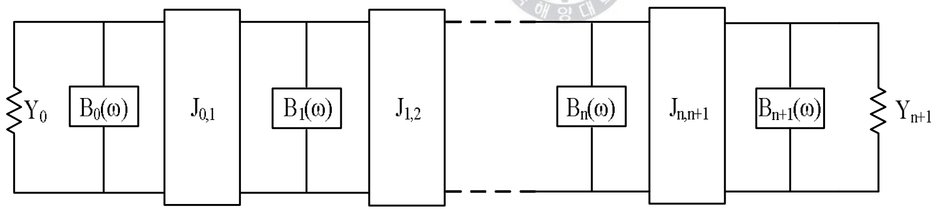

$B_n(\omega)$: Resonance circuit; $J_{n,n+1}$: Admittance inverter.

Fig.3.1 A generalized, bandpass filter circuit using admittance inverters.

There are a lot of circuits that operate as inverters. One of the simplest forms among these inverters is a quarter-wavelength transmission line. The admittance inverter parameter of the quarter-wavelength transmission line inverter will be $J = Y_0$, where

Y_0 is the characteristic admittance of the transmission line. Although the inverter properties are relatively narrow-band in nature, this quarter-wavelength line can be used without any problem as an admittance inverter in our proposed narrow band filters.

3.2 Size-reduced Bandpass Filter

We here use the above discussed quarter-wavelength transmission line inverters in our proposed filter. Given the bandpass filter model in Fig.3.1, a one-stage bandpass filter is proposed in Fig.3.2, where two LC resonant circuits functions as $B_1(\omega)$ and $B_2(\omega)$. Here the λ/4 transmission line admittance inverter is miniaturized using the method discussed above to get a very compact filter resulting in the circuit in Fig.3.2 (b). Here there are two inductors should be noticed in the resonant circuits at each side of the admittance inverter in Fig. 3.2 have been replaced by the coupled lines as discussed in last chapter. These two LC circuits are hidden but still function as resonators, which have reduced the number of needed lumped elements in the proposed filter. Therefore, the circuit can be used as the finally miniaturized one-stage bandpass filter.

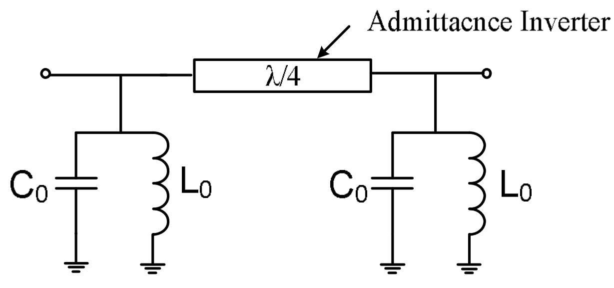

(a)

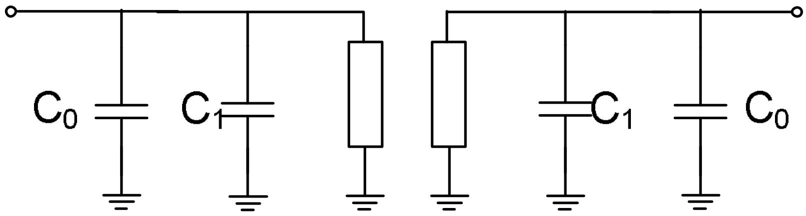

(b)

Fig.3.2 A one-stage bandpass filter based on the generalized filter model (a) and its miniaturized form (b).

Fig.3.3 gives the ADS model of the proposed size-reduced one- and two-stage filters. A three-stage filter can be made simply by connecting one more stage and is therefore omitted here. Two- and three-stage filters certainly have sharper skirt characteristics, but many stages usually lead to a relative larger insertion loss in fabrication. Therefore, a compromise method sometimes should be made between sharp skirt characteristics and small insertion loss. The simulation results of the 1- and 2-stages of the proposed bandpass filters have been given in Fig.3.4, and here we chose 7 degrees as the electrical length of the coupled lines.

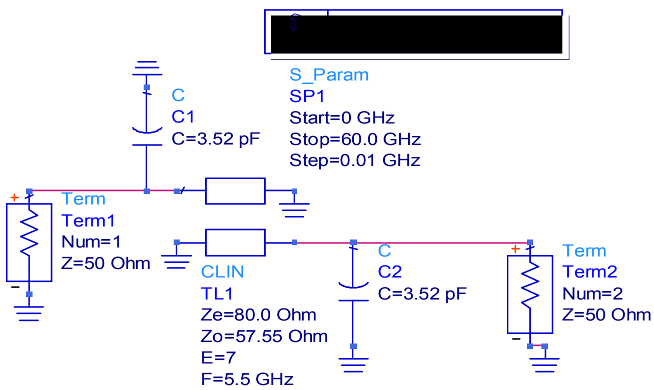

(a)

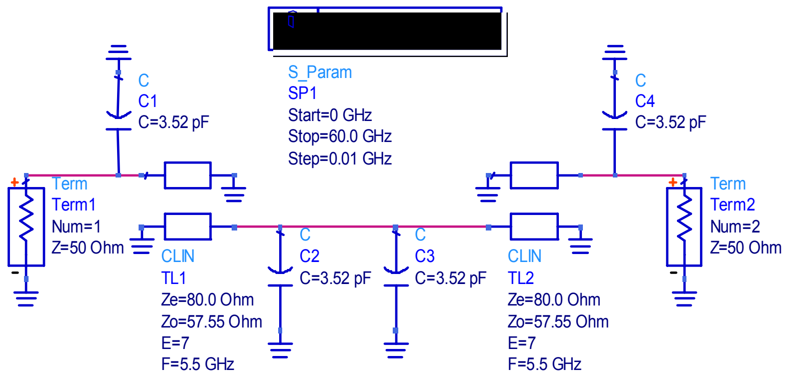

(b)

Fig.3.3 Model of the proposed one- and two-stage bandpass filter.

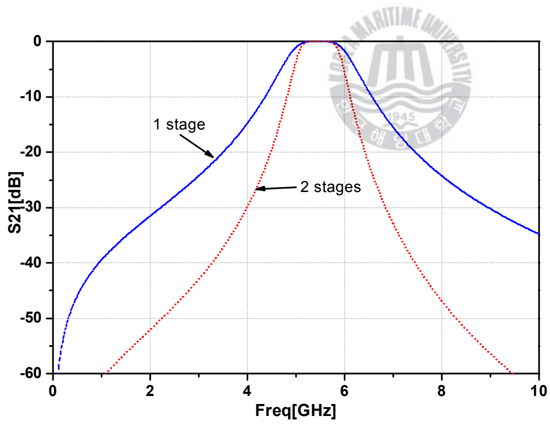

(a)

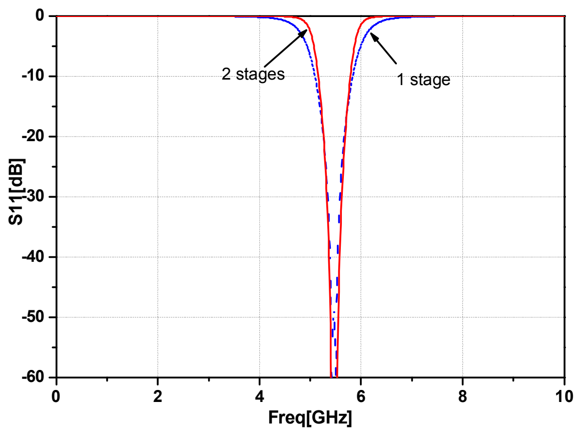

(b)

Fig.3.4 Simulation results of 1- and 2-stage filters for comparison of skirt characteristics: (a) Passband; (b) return loss.

Bandwidth is another important parameter of the bandpass filters in addition to insertion loss. The electrical length and coupling coefficient of the end shorted coupled lines are mainly two factors that can affect the bandwidth of the proposed bandpass filter. The bandwidth always varies as the electrical length of the coupled lines changes. The longer the length of the coupled lines, the larger the bandwidth is. In Fig.3.5, the quarter-wavelength transmission line has been miniaturized to 3, 5 and 7 degrees and the simulation results of ADS fully proved the correctness of this discussion. When we miniaturize the quarter-wavelength transmission lines, we can choose an appropriate electrical length to meet the bandwidth demand.

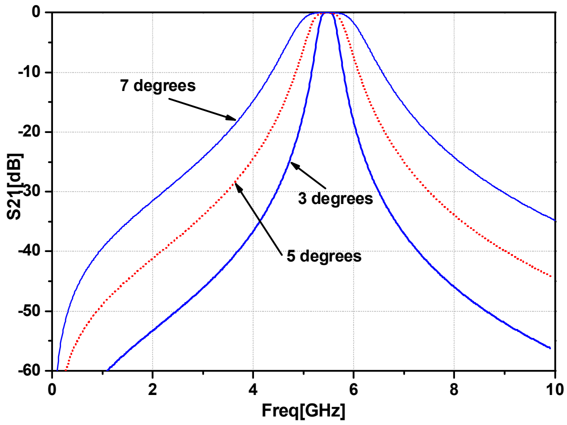

(a)

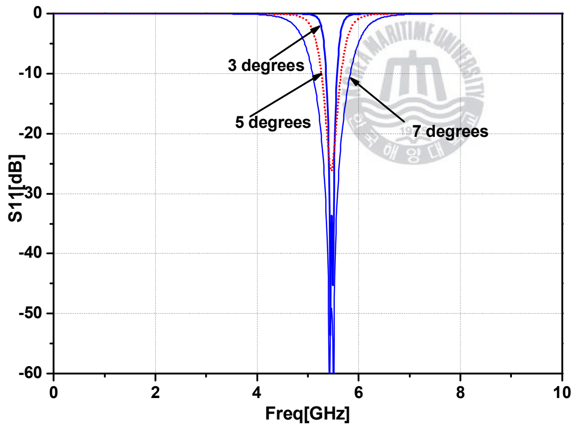

(b)

Fig.3.5 Different bandwidth according to different electrical length of the coupled lines: (a) Passband; (b) Return loss.

The coupling coefficient of the coupled lines is another factor that can affect the bandwidth of miniaturized filter. To prove this point, let's check the phase variation of the S_{21} parameter of the miniaturized quarter-wavelength transmission line firstly, which is given here as:

$$S_{21} = \frac{-y_{21}Y_0}{D_Y}.(-1) \tag{3.2}$$

Where

$$\begin{aligned}
&\Delta y = (y_{11} + Y_0)(y_{22} + Y_0) - y_{12}y_{21} \\
&y_{11} = y_{22} = -jY_{0e}\cot\theta - j\frac{Y_{0o} - Y_{0e}}{2}\cot\theta + jB \\
&y_{21} = y_{12} = -j\frac{Y_{0o} - Y_{0e}}{2}\cot\theta \\
&B = Y_{0e}\cot\theta + Y_0\cot\theta \\
&Y_0 = \frac{Y_{0o} - Y_{0e}}{2}
\end{aligned} \tag{3.3}$$

Y_{0o} , Y_{0e} are the odd and even mode admittance of the coupled lines respectively.

From equation (3.2), the minus value in the parentheses shows the $180°$ phase difference between the original quarter-wavelength transmission line and its equivalent miniaturized circuit, which was introduced when we equated the PI network to the end shorted coupled lines. y_{11} , y_{22} , y_{21} , y_{12} are the y-parameters of the equivalent circuit of the quarter-wavelength transmission line. At resonance frequency, equation (3.3) is satisfied when the characteristic admittance Y_{0e} of the end shorted coupled lines is equal to that of the shunt capacitance. With a straightforward analytical manipulation, the equation for the phase of S_{21} can be derived as

Phase of

$$S_{21} = \frac{3}{2}\pi + \tan^{-1} x_1 + \tan^{-1} x_2 \tag{3.4}$$

$$x_1 = \frac{B}{Y_0} - 2\cot\theta - \frac{Y_{0e}\cot\theta}{Y_0} \tag{3.5}$$

$$x_2 = \frac{B - Y_{0e}\cot\theta}{Y_0} \tag{3.6}$$

Near the center frequency, x_1 x_2 are expressed by $-\cot\theta$ and $\cot\theta$, respectively, using (3.3). The phase of S_{21} is -90° at the resonance frequency. If the frequency deviates from the center frequency, the relation $C_0\omega = Y_{0e}\cot\theta$ can not be satisfied and the phase of S_{21} starts to deviate from -90°. At this point, the most important item is to decrease the frequency sensitivity of the equivalent $\lambda/4$ transmission line. If Y_{0e} is small, the frequency sensitivity decreases because of the very small shunt value of $C_0\omega$ in the artificial resonance circuit. The coupling coefficient K is:

$$K = \frac{Y_{0o} - Y_{0e}}{Y_{0o} + Y_{0e}} \tag{3.7}$$

From (3.7), the following relation is obtained:

$$Y_{0e} = \frac{1-K}{1+K} Y_{0o} \tag{3.8}$$

In (3.8), when the coupling coefficient is nearly unity Y_{0e} is very small. The 90° phase shift near the center frequency is independent of the coupling coefficient K. The larger the coupling coefficient K, the broader the bandwidth of the bandpass filter, as illustrated by Fig. 3.6, where the electrical length of the coupled lines is chosen as 7° and two stages are used.

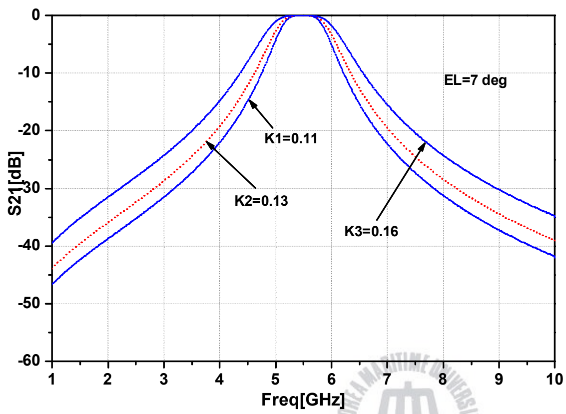

(a)

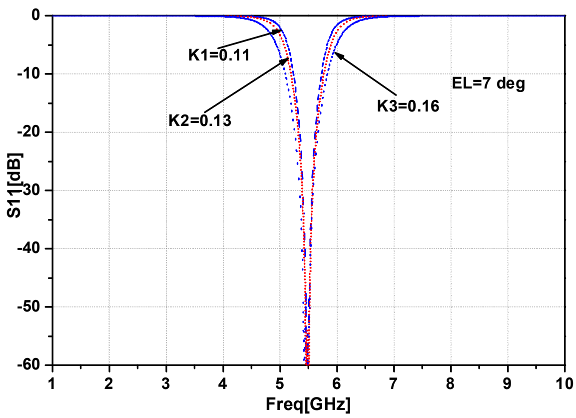

(b)

Fig.3.6 Relation between the bandwidth and coupling coefficient of the coupled lines: (a) Passband and (b) Return loss.

This miniaturized filter is a kind of bandpass filter, but its structure is different from the traditional one mentioned in the introduction part of this paper. Before concluding the design theory of the bandpass filter, a comparison is made here between the proposed bandpass filter and the traditional one.

Firstly, a small inter-stage microstrip transmission line is used between two resonators (stages) in the modified bandpass filter to prevent the unwanted coupling between the neighboring two resonators. At the same time, the insertion of the short transmission line does not affect the active characteristics of the modified bandpass filter, and performs good effect on the result.

Secondly, there are resonance circuits at both the input and output ports. In a traditional bandpass filter, the end shorted transmission lines used as input and output are equivalent to shunt inductors. A very small length of the input and output transmission line will lead to a very small inductance and therefore an extremely large impedance, and the input signal will not be able to flow at all. This has hindered the miniaturization of the traditional bandpass filter. Usually the length of transmission lines in the traditional bandpass filter is about $\lambda/8$. However, in the modified one, the problem is solved with the resonant structure used at both the input and output ports. At the same time, two more poles are added because of the added resonant circuits, which contribute to the sharp shirt characteristics of the modified bandpass filter.

Finally, the size of the modified bandpass filter can be extremely miniaturized according to $Z' = \frac{2Z_{0e}Z_{0o}}{Z_{0e} - Z_{0o}}$, who's potential has been neglected in traditional bandpass filters. For a given Z_0, the electrical length of the parallel coupled lines can be made very small, so long as we choose $Z_{0e} \approx Z_{0o}$.

As shown above, the main key factors to affect the bandwidth of the bandpass filter are the electrical length and coupling coefficient of the end shorted coupled transmission line. The longer the length of the coupled transmission line, the larger the bandwidth is. The bigger of the coupling coefficient K, the larger the bandwidth is.

Chapter 4 Simulation and Measurement Results

In this paper, a two stages GaAs process band-pass filter for 5GHz band WLAN applications is designed. In the two stage structure, band pass filter behaves as 3 pole topologies like Fig.2.4, because an admittance inverter per one stage includes two resonators. The electrical length of coupled lines is set to 7^{o} degrees and Z=410.3 Ω is derived from equation (2.3). This high impedance can be achieved from equation (2.6) with Zoe ≈ Zoo. To solve equation (2.6), there is a one equation and the two unknowns Zoe and Zoo. Arbitrary Zoe can be selected and then, Zoo finally is derived. The selection of Zoe is related to the bandwidth of quarter transmission line with a resonance circuit.

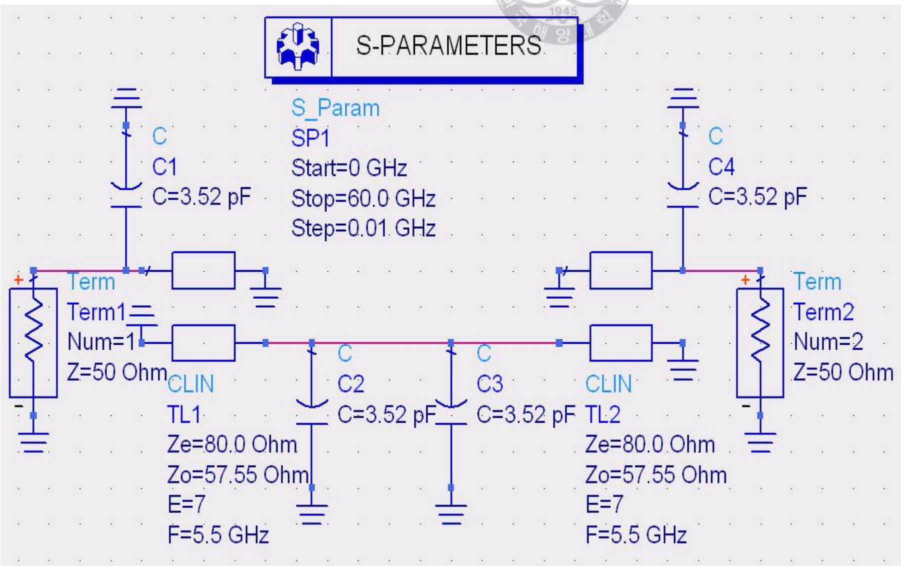

Fig.4.1 The simulation circuit by ADS.

For simple design, two same resonators are cascaded. If conventional design technique-Butter worth or Chebychev, is used, components (MIM capacitors, and the conditions of coupled lines) of each section are different. In the extremely miniaturized circumstances, it is very difficult to fabricate each component exactly like designed one because of unexpected coupling between components. This specified response is achieved through circuit simulation by Agilent ADS with component values Zoe=80 Ω, Zoo=60 Ω, and four capacitors C=3.52 pF. The physical dimensions of coupled lines are determined by Zoe and Zoo. Fig.4.2 shows the ADS simulated result. The wide band characteristic expresses good spurious stop band.

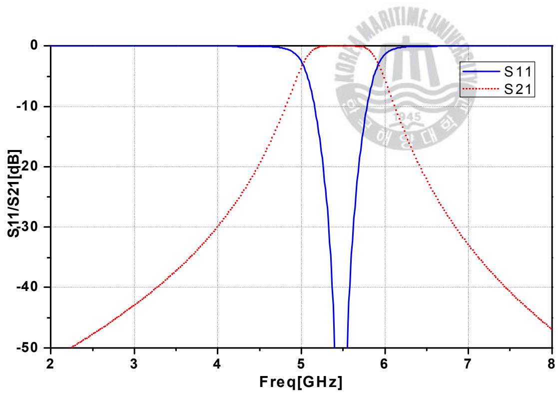

(a)

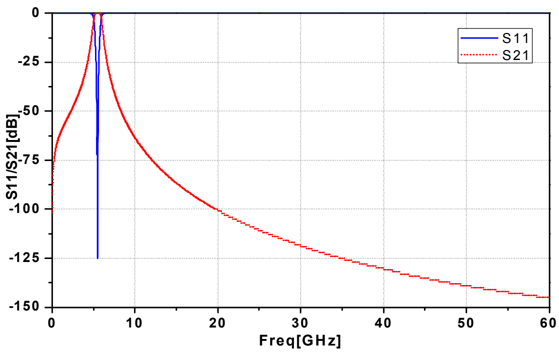

(b)

Fig.4.2 Simulation result (a) The narrow band characteristic. (b) The broad band characteristic.

Subsequently, we simulated the circuit with ansoft HFSS V9 to accomplish the effect of the overall response. After calculation and optimization, the final circuit of HFSS is shown by Fig.4.3 (a) and (b). The area size of band pass filter is about 0.54×0.78 mm^2. As far as authors know, this size is nearly the most miniaturized filter reported to date at 5GHz.

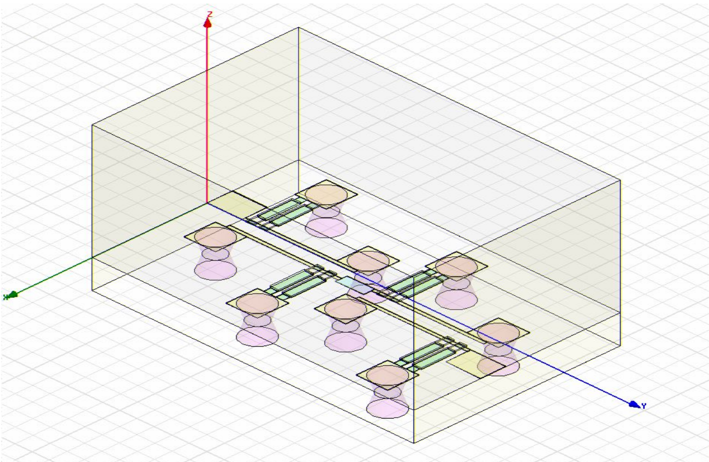

(a)

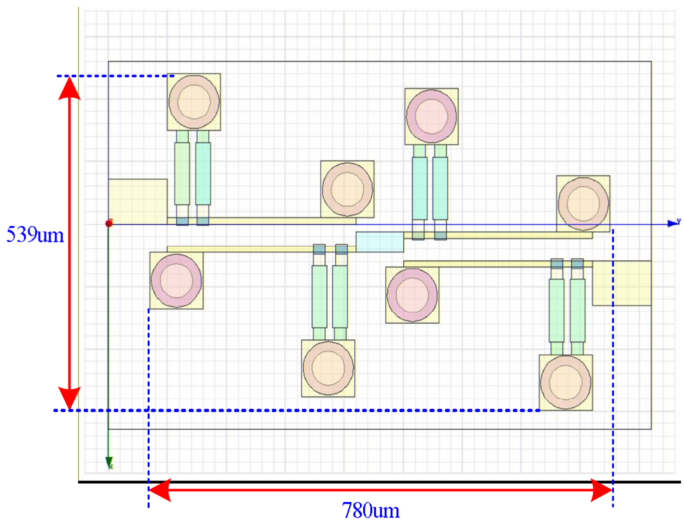

(b)

Fig.4.3 The simulation circuit by HFSS.

After finishing the simulation, we draw the layout circuit in ADS by using the design kit of Knowledge*on semiconductor company. Fig 4.4 shows the layout circuit photograph and the microphotograph of the real circuit.

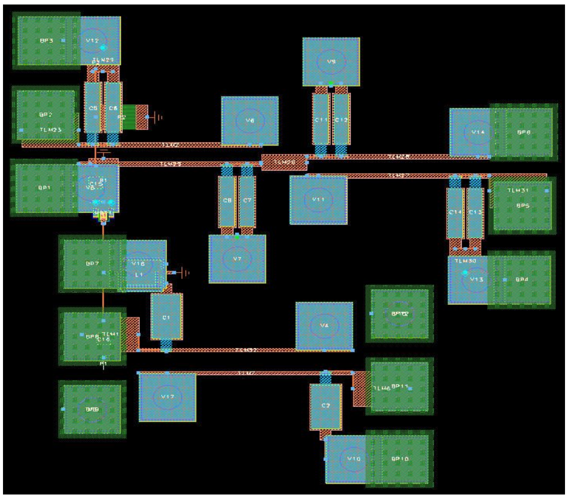

(a)

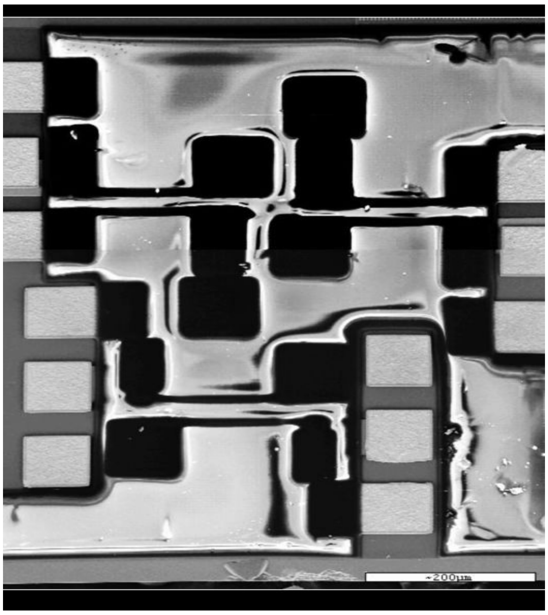

(b)

Fig.4.4 (a) Layout circuit by ADS.

(b) One and two stages Microphotograph of MMIC.

Compared with the others filter fabricated technology process, the main advantage of this kind of filter is the extremely miniaturized size. A size comparison of the different types of compact filters is show in Fig4.5. Here we got a band pass filter from Japan SOSHIN electric company, which type is HMD851H. Its frequency is 5487.5 MHz, and size is 2x1.25x1.0 mm^3. So it is much bigger than ours.

Type	Author	f_0 (MHz)	Er	E.L.	Physical Size (mm^2)
Slow-wave	Lung-Hwa Hsieh	2000	10.2	61	21.245×6.691
SIR	Hualiang Zhang	2400	4.5	90	20.1×20.4
Ceramic Combline	Huiwen Yao	915	38.2	45	3.0×3.0
Proposed	Shiwei Shan	5500	3.56	7	0.54×0.78

E.L.: The electrical length of a resonator in degree.

Er: The dielectric of the PCB used for fabrication.

Fig.4.5 The size comparison of different types of compact bandpass filter(one resonator).

Fig.4.6 shows the HFSS simulation results. According to Fig.4.6, the effects of eight via holes in the filter circuit can be ignored. In Fig.4.3, there is an inter-stage transmission line 80 um to prevent the unexpected coupling between two resonators. This concept is well explained by [12]. Although HFSS has been used to find the proper capacitor value in the simulation work, it is MIM capacitor that was employed in the HFSS model for simulation. Capacitance of the lumped capacitor available in the lab is a little different from that of the MIM capacitor, leading to a little deviated center frequency.

In the HFSS simulation results, there are two attenuation poles appear. It can be expected because of the boundary and excitation setting in HFSS, the inserted inter-stage transmission line and the coupling between the elements of circuit. When we simulate one stage as a unit circuit, there are two poles show up. But if we cascade it to a two stages circuit, it probably become a little different from the one stage circuit owing to the size of the inter-stage transmission line. The number of attenuation poles is different after changing the size of inter-stage transmission line. For the purpose of optimization, the final results show in Fig.4.6.

Compared with the measure result, there is a little different between them because of the design and simulation error, fabrication process accuracy and artificial error in the measurement.

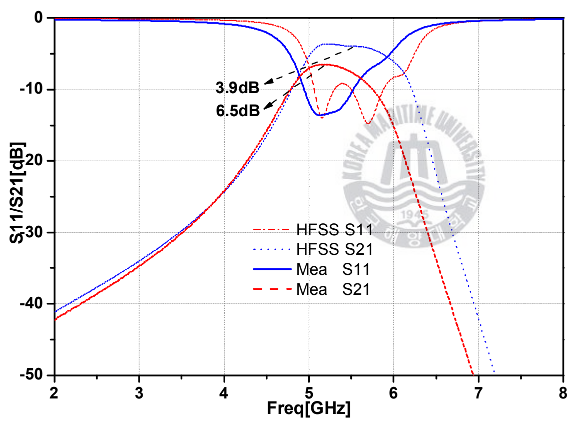

(a)

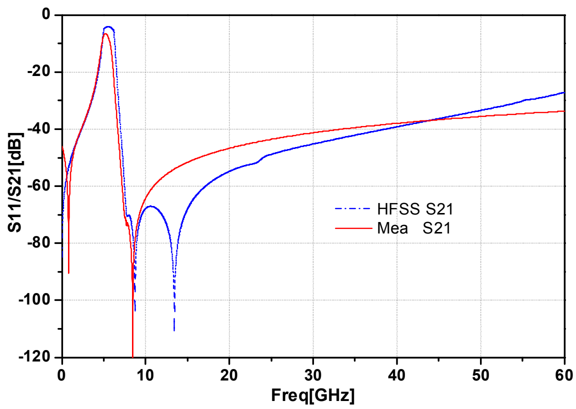

(b)

Fig.4.6 The comparison measurement data with simulation (a) The narrow band characteristic. (b) The broad band characteristic.

Fig.4.6 compares the measured data with HFSS simulated results and it is clear that there is good agreement with the two results. In the measurement results, the pass band has a maximum insertion loss 6.5dB with 0.9 GHz bandwidth, from 4.8GHz to 5.71GHz and 13dB return loss.

The measured center frequency is shifted to lower frequency by 0.15 GHz. It is presumed to be resulted from MIM capacitance fabrication accuracy and simulation error. The bandwidth of measured data is shrunk from 1.15 GHz into 0.9 GHz. Simultaneously, the insertion loss also, gets worse from 3.9 dB to 6.5 dB. The loss will be recovered if bandwidth is designed to be wide because the wider bandwidth is, the better insertion loss is.

The lower band suppression was > 24dB form 0 – 4 GHz and the upper spurious stop band is >35dB up to 60 GHz. This ultra-wide stop band characteristic is a special advantage, comparing the ceramic or SAW filters.

Chapter 5 Conclusion

A very compact GaAs band-pass filter using combination of diagonally end-shorted coupled lines and lumped capacitors was proposed in this paper. This very compact structure has many attractive advantages: very small size, low cost, easy-to-design, easy-to-fabricate, and broad rejection bandwidth and so on. This type of filters has a wider upper stopband characteristic over 35 dB up to 60 GHz. Using this method, the size of band pass filter at 5 GHz band with planer GaAs process for RF single transceiver chip can be controlled arbitrarily in theory and reduced to just a few degrees. After fabrication, area size of the real circuit is about 0.42 mm^2 .

Measured results of the fabricated Bandpass filter matched very well with the simulated performances, which verified the validity of this size-reduction method. This approach can be further extended and utilized in the various fabrication processes owing to planer structure.

References

[1] M. Makimoto and S. Yamashita, “Bandpass filters using parallel coupled strip-line stepped impedance resonators,” *IEEE Trans. Microwave Theory Tech.*, vol. MTT-28, no. 12, pp. 1413–1417, Dec.1980.

[2] A. Djaiz and T. A. Denidni, “A new compact microstrip two-layer bandpass filter using apertured-coupled SIR-hairpin resonators with transmission zeros,” *IEEE Trans. Microwave Theory Tech.*, vol.54, no.5, pp.1929-1936, May.2006.

[3] M. Sagawa, K. Takahashi, and M. Kakimoto, “Miniaturized hairpin resonator filters and their application to receiver front-end MICs,” *IEEE Trans. Microwave Theory Tech.*, vol. 37, pp. 1991-1997, 1989.

[4] J. Hong and M. J. Lancaster, “Theory and experiment of novel microstrip slow-wave open- loop resonator filters,” *IEEE Trans. Microwave Theory Tech.*, vol. 45, pp. 2358-2365, 1997.

[5] C. W. Tang, Y. C. Lin and C. Y. Chang, “Realization of transmission zeros in combline filters using an auxiliary inductively coupled ground plane,” *IEEE Trans. Microwave Theory Tech.*, vol.51, no.10, pp.2112-2118, Oct,. 2003.

[6] A. Kundu and N. Mellen, “Miniaturized Multilayer Bandpass Filter with multiple Transmission Line Zeros”, *IEEE MTT-S Int. Microwave Symp. Dig.*, pp. 760-763, June 2006.

[7] A. Hussain, *Advanced RF Engineering for Wireless systems and Network*, Wiley, pp.262, 2005.

[8] C. Tzuang, H. Wu, H. Wu and J. Chen, “A CMOS Miniaturized C-Band Active Band pass Filter,” *IEEE MTT-S Int. Microwave Symp. Dig.*, pp. 772-775, June 2006.

[9] Jia-Sheng Hong and M.J. Lancaster, “Microstrip Filters for RF/Microwave Applications,” *Advanced Materials and Technologies*, pp.217-219, 2001.

[10] I. Kang and K. Wang, “A broadband rat-race ring coupler with tight coupled lines,” *IEICE Communications*, vol.e88-B, no.10, 4087-4089, 2005.

[11] G. Matthaei, L. Young and E.M.T. Jones, *Microwave Filters, Impedance Matching Networks and Coupling Structures*, Artech House Inc., Norwood, MA 1980, p. 433.

[12] I. Kang and H. Xu, “An extremely miniaturized microstrip bandpass filter,” *Microwave Journal* (be accepted).

Acknowledgement

I would like to deliver my heartfelt gratitude to many people who have offered me help in both my study and daily life during the past two years in Korea. Without their generous supports and assistance, it would have been impossible for me to finish my study, even my dissertation.

I can not be thankful enough to my advisor, Professor In-ho Kang, who has wide knowledge, strict research attitude and enthusiasm in work deeply impressed me and taught me what a true scientific research should be. I am also thankful to the other Professors of our department for their supports and guidance on this work, who are Professor Dong Il Kim, Professor Kyeong-Sik Min, Professor Hyung Rae Cho, Professor Ki Man Kim, Professor Ji Won Jung, Professor Young Yun, Professor Joon hwan Shim and Professor Dong Kook Park in Department of Electronic and Communication Engineering..

I also want to say thanks to my senior Mr. Rui Li, Mr. Kai Wang Miss Haiyan Xu and my laboratory member Mr. Xuguang Wang for their timely and unselfish help. They not only help me with my study work, but also let me enjoy the friendly work environment. My heartfelt thanks are also due to my friends in Microwave and Antenna lab, Mr. Seo Yong Gun and others who offered me great helps in my experiments.

Finally, I would like to express my sincere thanks to Professor

Yingji Piao, Mr. Zheng Li and Miss Dan Li at Qingdao University of China. Without their recommendation, it is impossible for me to get the opportunity to study in Korea.